Optics Letters

High-power, 1-ps, all-Yb:YAG thin-disk regenerative amplifier

Hanieh Fattahi,[1,2,*] Ayman Alismail,[2,3] Haochuan Wang,[1,2] Jonathan Brons,[1] Oleg Pronin,[1,2] Theresa Buberl,[4] Lénárd Vámos,[2,5] Gunnar Arisholm,[6] Abdallah M. Azzeer,[3] and Ferenc Krausz[1,2]

[1]Max-Planck Institut für Quantenoptik, Hans-Kopfermann-Str. 1, D-85748 Garching, Germany
[2]Department für Physik, Ludwig-Maximilians-Universität München, Am Coulombwall 1, D-85748 Garching, Germany
[3]Physics and Astronomy Department, King Saud University, Riyadh 11451, Saudi Arabia
[4]Techincal University of Munich, James-Franc- Str. 1, D-85748 Garching, Germany
[5]Wigner Research Center for Physics, Konkoly-Thege Miklós út 29-33, H-1121 Budapest, Hungary
[6]FFI (Norwegian Defence Research Establishment), P.O. Box 25, NO-2027 Kjeller, Norway
*Corresponding author: hanieh.fattahi@mpq.mpg.de

Received 18 January 2016; revised 9 February 2016; accepted 9 February 2016; posted 11 February 2016 (Doc. ID 257223); published 8 March 2016

We report a 100 W, 20 mJ, 1-ps, all-Yb:YAG thin-disk regenerative amplifier seeded by a microjoule-level Yb:YAG thin-disk Kerr-lens mode-locked oscillator. The regenerative amplifier is implemented in a chirped pulse amplification system and operates at an ambient temperature in air, delivering ultrastable output pulses at a 5 kHz repetition rate and with a root mean square power noise value of less than 0.5%. Second harmonic generation of the amplifier's output in a 1.5 mm-thick BBO crystal results in more than 70 W at 515 nm, making the system an attractive source for pumping optical parametric chirped pulse amplifiers in the visible and near-infrared spectral ranges.

OCIS codes: (140.0140) Lasers and laser optics; (140.3480) Lasers, diode-pumped; (140.3515) Lasers, frequency doubled; (140.3615) Lasers, ytterbium.

http://dx.doi.org/10.1364/OL.41.001126

Attosecond technology has provided direct time-domain access to the motion of electrons on the atomic time scale [1]. However, there are many exciting phenomena with significant technological and scientific implications waiting to be observed and controlled once attosecond pulses with higher flux and energy become available. Few-cycle pulses of Ti:Sa-based chirped pulse amplification (CPA) systems have been the workhorse for the generation of attosecond pulses for more than a decade [2], but their peak and average powers for few-cycle pulses are limited. As the cutoff frequency in high harmonic generation (HHG) is proportional to the energy and square of the wavelength of the driving pulses [3,4], HHGs can be dramatically changed if short pulses at a higher energy and a longer wavelength are available. Unlike CPA lasers, optical parametric chirped pulse amplifiers (OPCPA) are scalable in average and peak power and flexible in terms of the central frequency of the amplified spectrum [5,6], but their realization demands high peak-power pump lasers.

Among the currently available laser media, Yb-doped materials are most promising for scaling the average and/or peak power of few-picosecond pulses [7–11], and are therefore unrivaled pump sources for OPCPA. The medium can be pumped with cost-effective diode lasers and because of the absence of excited-state absorption, good thermal conductivity, and cubic crystal structure, they show superior performance in thin-disk geometry. Here, efficient heat transfer takes place through a heat sink attached to the laser gain medium. Due to this cooling concept, the crystal size in thin-disk amplifiers can be scaled easily, which holds promise to reach pulses with joule-level energy and kilowatt-scale average power [12,13]. However, the amplified energy is limited by amplified spontaneous emission [14].

Combining the Yb:YAG gain medium in thin-disk geometry with a CPA allows the scaling of the energy of near-1 ps pulses while keeping the B-integral in the amplifier low. This results in pulses with excellent temporal and spatial profiles, which are important to achieving high efficiency and good beam and pulse quality in an OPCPA.

In this work, we show an all-Yb:YAG thin-disk regenerative amplifier seeded with a Yb:YAG thin-disk Kerr-lens mode-locked (KLM) oscillator delivering 20 mJ, 1 ps pulses at 100 W of average power with excellent short- and long-term stability. Figure 1 outlines the scheme of the system. As described in [15], a higher seed energy results in less accumulated nonlinear phases in regenerative amplifiers. Therefore, a Yb:YAG thin-disk KLM oscillator was developed to provide a high input seed energy for the regenerative amplifier.

The front-end oscillator was designed to meet certain parameters that are critical in reaching the optimum day-to-day performance of the attached amplifier system.

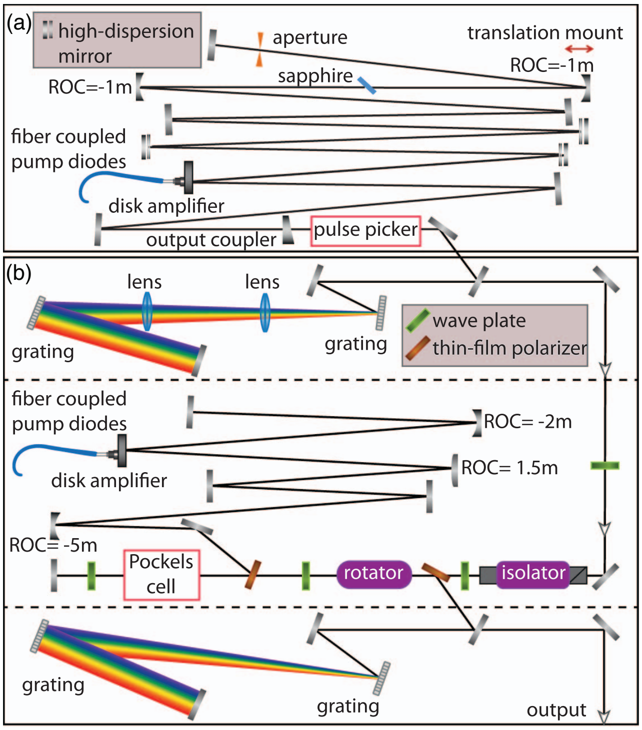

Fig. 1. Schematic layout of the Yb:YAG thin-disk regenerative amplifier. (a) The fiber-coupled diode-pumped KLM thin-disk Yb:YAG oscillator delivers 350 fs pulse at an 11 MHz repetition rate and 2 μJ of energy. A pulse picker is used to reduce the repetition rate to 5 kHz at the input of the amplifier. (b) The input seed pulses are temporally stretched before entering the regenerative amplifier. The amplifier cavity contains a fiber-coupled, diode-pumped, Yb:YAG thin-disk gain medium. The amplified pulses are coupled out using a Pockels cell and subsequently compressed in a reflective dielectric grating compressor. ROC: radius of curvature.

Among them are microjoule-level pulse energy, sub-picosecond pulse duration, and low beam-pointing fluctuations, as well as good thermal and mechanical stability. Today, the highest pulse energy directly from mode-locked oscillators has been generated with thin-disk technology, mainly by employing Yb:YAG as a gain material [16–18].

The cavity setup of the oscillator is shown in Fig. 1(a). The linear cavity is bounded by a wedged output coupler with 13% transmission and a highly reflective end plane mirror, and has a total length of about 13 m. Light amplification is performed by a flat Yb:YAG thin disk that works in reflection and is pumped by fiber-coupled laser diodes at a 940 nm wavelength. Solitonic pulse shaping is supported by a net intra-cavity group-delay dispersion (GDD) of $-18,000\ \mathrm{fs}^2$ per round trip, introduced by three high-dispersion mirrors. The necessary loss modulation for stable pulse generation is provided by a 1 mm-thick sapphire Kerr medium placed between two concave focusing mirrors (−1 m radius of curvature) in combination with a copper aperture and the soft aperture of the gain. Mode locking is initiated by perturbing a concave mirror on a translation stage.

Frequency-resolved optical gating based on second harmonic generation (SHG-FROG) employing a 100 μm BBO crystal is used to characterize the oscillator pulses. The output pulses are transform limited with a duration of 350 fs at the

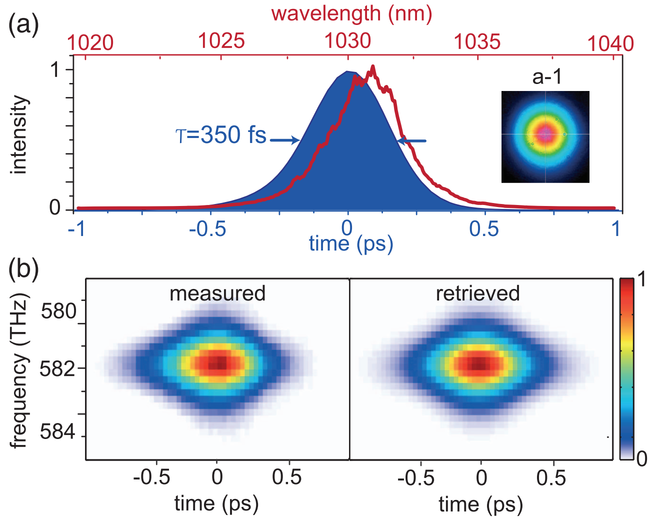

Fig. 2. (a) Oscillator's output spectrum at 25 W of average power (red) along with the retrieved temporal intensity (blue). Inset: transverse intensity profile of the oscillator. (b) Measured and retrieved SHG-FROG spectrograph of the oscillator. G_{error}: 6.8×10^{-3}.

FWHM, each carrying about 2 μJ of energy (Fig. 2). During the course of a workday, the average output power is 25 W, while the root mean square (rms) intensity noise on a photodiode is less than 1% in a 1 Hz–13 MHz spectral window. The rms of the beam pointing fluctuations of the oscillator is less than 0.6% of the beam size over a measurement time window of one hour. The thermal stability of the system is sufficient for near turn-key operation such that alignment of the oscillator is not required on consecutive workdays. The most important parameters of the oscillator, such as the spectral intensity, transverse spatial intensity, and temporal intensity profile, are shown in Fig. 2.

The repetition rate of the pulse train delivered by the oscillator is reduced to 5 kHz before seeding the regenerative amplifier using a pulse picker containing a 25 mm-thick BBO crystal. A pair of gold gratings is used to stretch the high-energy seed pulses. The grating setup provides a GDD of −500 ps/nm. After the stretcher, the seed pulses have 1 μJ of energy and a 2.92 nm spectral bandwidth (FWHM). The stretched pulses are sent to the cavity of the regenerative amplifier, which contains a Faraday rotator to separate the incoming and outgoing pulses, and a Pockels cell with a 20 mm-thick BBO crystal and a clear aperture of 10 mm × 10 mm to couple out pulses from the amplifier.

An approximately 100 μm-thick Yb:YAG thin disk provided by TRUMPF Laser GmbH is used as the gain medium. The 9 mm-diameter disk has a radius of curvature of −2 m and is doped about 7%. The disk module is thermally back-contacted to a water-cooled diamond heat sink, which is connected to a chiller and is pumped with continuous-wave (cw) fiber-coupled diodes at a wavelength of 940 nm with a near-flat-top beam profile with a diameter of 3.5 mm.

At 280 W of cw pumping and after 87 round trips, 130 W of average power is achieved corresponding to an optical-to-optical efficiency of 47%. The M^2 measurement indicates that $M_x^2 = 1.08$ and $M\ 2_y = 1.07$ for the amplified beam. The beam profile and the spectrum of the amplified pulses are

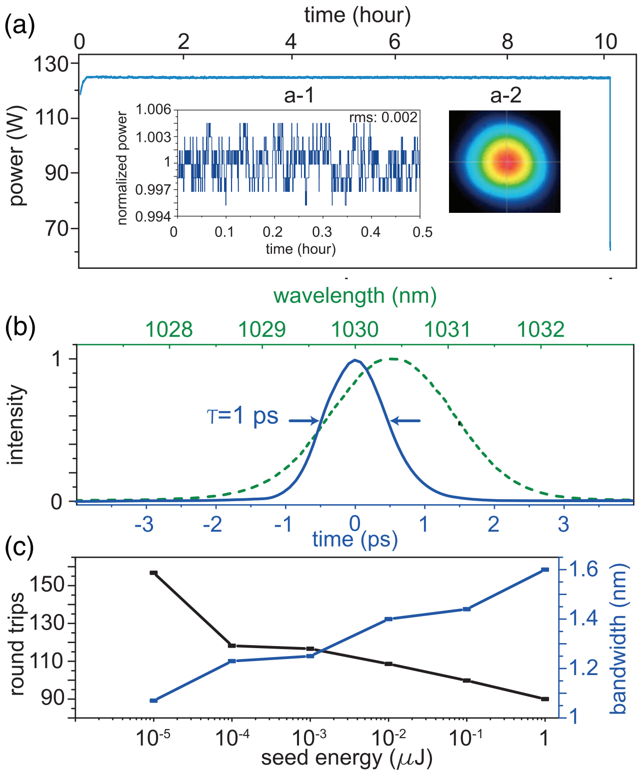

Fig. 3. (a) Average power of the Yb:YAG thin-disk laser over 10 h of continuous operation, measured with an OPHIR powermeter head (L1500W-BB-50-V2). Inset: (a-1): power normalized to its mean value in a half an hour time window. (a-2): Beam profile of the amplified pulses. (b) Output spectrum (green) and the retrieved temporal profile (blue) of the laser pulses at 100 W average power after the grating compressor. (c) Spectral bandwidth (FWHM) of the amplified pulses, and the required round trips at 300 W of pump energy versus seed energy.

shown in Figs. 3(a) and 3(b). The amplifier is operated in saturation and delivers pulses with high stability: the rms of the peak-to-peak energy fluctuations is measured to be less than 1% over a period of 2 s, while the amplifier shows outstanding average power stability over 10 h of uninterrupted operation [Fig. 3(a)]. The keys to this performance include aggressive gain saturation and optimization of the power supply of the laser diodes and the cooling system for the most stable operation.

The amplified pulses are sent to a reflective multilayer dielectric grating pair (line density of 1740 l/mm) for temporal compression with an overall throughput efficiency of 80%. Figure 3(b) shows the retrieved temporal intensity profile of the amplifier pulses, measured by using an SHG-FROG and yielding a pulse duration of 1 ps at the FWHM, which is near the 0.98 ps transform limit.

We also measured the spectral bandwidth of the amplified pulses versus the seed energy while the pump energy was fixed and the number of round trips in the amplifier was adjusted to obtain the highest output energy for each seed energy. The seed energy was reduced by neutral density filters. Figure 3(c) shows spectral bandwidth of the amplified pulse (FWHM) and the required number of round trips versus the seed energy. It is clearly seen that gain narrowing reduces the bandwidth of the amplified pulses when the seed energy is reduced. For seed energy below 10 pJ, the amplifier was unstable and it was not possible to overcome period doubling by increasing the round trip time in the cavity.

The performance reported above renders this system an ideal candidate for pumping OPCPA systems in the near-infrared and (after frequency upconversion) visible spectral ranges. Fulfilling the conservation of energy in the visible OPCPA requires the generation of low-order harmonics of the amplifier. Among the numerous available materials for SHG, critically phase-matched LBOs and BBOs are the best candidates due to their fairly high nonlinear coefficients and damage thresholds. BBO has a higher nonlinearity than LBO, but a larger spatial walk-off and it is limited in the available aperture.

The SHG stage was designed by simulating SHG in BBO and LBO using the SISYFOS code [19]. As the measured pump pulses in space and time have a near-Gaussian profile, we assumed a Gaussian spatiotemporal structure for the pump pulses. In the LBO, the phase-matching angle (θ) was 13.7° and d_{eff} was 0.819 pm/V, and in the BBO, they were $\theta = 23.4°$ and 2 pm/V, respectively. The Sellmeier coefficients were taken from [20,21].

Figure 4(a) shows the simulated energy of the SHG versus the crystal length for 1 ps pulses (FWHM) centered at 1030 nm with a pulse energy of 20 mJ and a peak intensity of 100 $\mathrm{GW/cm^2}$ in type-I BBO and LBO crystals. In the case of the BBO crystal, the SHG reaches saturation in a 1.5 mm-thick crystal because a longer crystal back conversion from the second harmonic to the fundamental pulse takes place. It can be seen that because of the lower nonlinearity of the LBO as compared to the BBO, the saturation of the SHG in the LBO occurs at twice the thickness of the BBO. However, due to the smaller spatial walk-off between the second harmonic beam and the fundamental beam in the LBO, a conversion efficiency similar to the BBO can be achieved [22].

To find the optimum operation regime, SHG-XFROG measurements of pulses at 515 nm and different efficiencies were performed, where the 1 ps pulses of the amplifier were used as the gate pulse. For simplicity, this measurement was conducted in a test SHG stage, containing a 1.5 mm-thick BBO crystal, but with using only 0.5 mJ pulse energy from the amplifier. The peak intensity on the crystal was adjusted to operate the SHG stage in saturation [Fig. 4(b), black curve].

Figure 4(c) compares the retrieved spectral intensity of the experimental second harmonic pulses at different efficiency points indicated on the black efficiency curve of Fig. 4(b) as A, B, and C. For 50% conversion efficiency, the second harmonic pulses have a pulse duration of 0.89 ps, due to pulse shortening based on the χ^2 effect. At higher efficiencies, higher-order spectral phase and spectral broadening is observed. As is shown in Fig. 4(c), at point C, the spectrum is modulated and a dip appears, owing to the back conversion of energy from second harmonic pulses to fundamental pulses. Nevertheless, these chirped second harmonic pulses still maintain a good spatial and temporal quality.

Equipped with this information, the accumulation of the nonlinear phase in the experimental SHG stage was minimized by using a 1.5 mm-thick BBO crystal for the frequency doubling of the full output of the amplifier. The pump beam size was adjusted to reach the peak intensity of 80 $\mathrm{GW/cm^2}$, which resulted in SHG efficiency of 70%, maintaining an excellent beam quality in both space and time [Fig. 4(b), green curve]. The second harmonic pulses have 70 W of average power, and

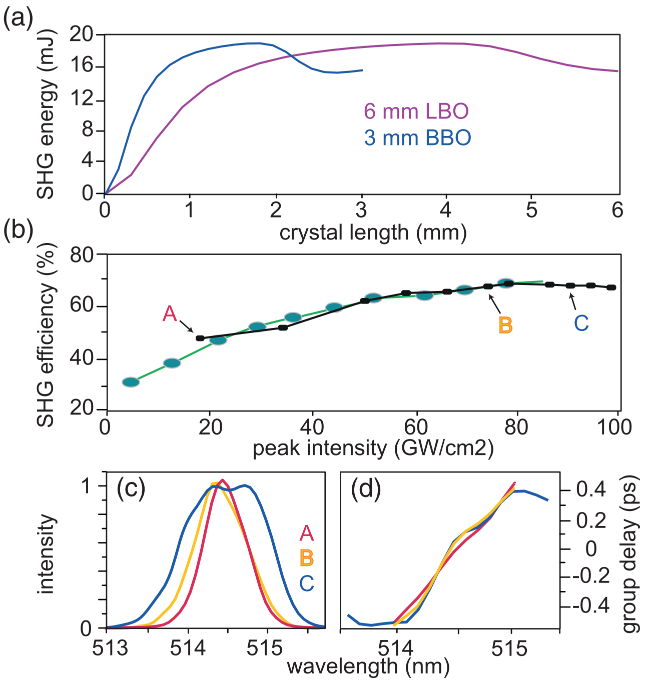

Fig. 4. (a) Simulated SHG efficiency versus crystal length in a 3 mm-thick BBO and 6 mm-thick LBO crystal. (b) Experimental SHG energy versus input pump energy in a 1.5 mm BBO crystal using 0.5 mJ (black curve) and 20 mJ (green curve) of the amplifier's energy. (c) Retrieved spectral intensity and (d) group delay of XFROG measurements of SHG at different efficiencies. Red, orange, and blue curves correspond to points A, B, and C on SHG efficiency curve (black curve in part b).

no phase mismatch due to the thermal effect or the degradation of the crystal is observed.

In conclusion, we have demonstrated an all-Yb:YAG-thin-disk laser system. By using a microjoule-scale, sub-400 fs KLM oscillator as the front end of the Yb:YAG thin-disk regenerative amplifier, the required number of round trips in the amplifier, and hence the spectral narrowing of the amplified pulses, is greatly reduced as compared to previous experiments [23]. This allows the amplification of each pulse seeded into the amplifier (as opposed to the reported period doubling [24]), and substantially improves the stability of the output pulses. As our previous study showed, higher seed energy also reduces the accumulated nonlinear phase and therefore improves the temporal phase of the amplified pulses [15].

The system delivers 1 ps pulses (FWHM) with 20 mJ energy at a 5 kHz repetition rate after the grating compressor. Frequency doubling of the amplified pulses in a simple SHG stage consisting of a 1.5 mm-thick BBO crystal results in more than 70 W of average power at 515 nm with the optical-to-optical efficiency of 70%. The turn-key performance of the amplifier combined with the demonstrated outstanding stability enables the generation of a stable, broadband supercontinuum from the same laser that pumps an OPCPA. This eliminates the need for temporal synchronization of seed and pump pulses, and together with passive carrier-envelope phase stability [24–26], it can lead to a new generation of high-energy, few-cycle OPCPA systems for exploration of new regimes in HHG and attosecond science.

Acknowledgment. We would like to thank Roswitha Graf, Martin Gorjan, Zsuzsanna Major, Moritz Ueffing, and Thomas Nubbemeyer at the Laboratory of Extreme Photonics (LEX) and Thomas Metzger and Dirk Sutter from TRUMPF Laser GmbH for their support.

REFERENCES

1. M. Hentschel, R. Kienberger, C. Spielmann, G. A. Reider, N. Milosevic, T. Brabec, P. Corkum, U. Heinzmann, M. Drescher, and F. Krausz, Nature **414**, 509 (2001).
2. A. L. Cavalieri, E. Goulielmakis, B. Horvath, W. Helml, M. Schultze, M. Fieß, V. Pervak, L. Veisz, V. S. Yakovlev, M. Uiberacker, A. Apolonski, F. Krausz, and R. Kienberger, New J. Phys. **9**, 242 (2007).
3. W. Schweinberger, A. Sommer, E. Bothschafter, J. Li, F. Krausz, R. Kienberger, and M. Schultze, Opt. Lett. **37**, 3573 (2012).
4. T. Popmintchev, M.-C. Chen, D. Popmintchev, P. Arpin, S. Brown, S. Alisauskas, G. Andriukaitis, T. Balciunas, O. D. Mücke, A. Pugzlys, A. Baltuska, B. Shim, S. E. Schrauth, A. Gaeta, C. Hernández-García, L. Plaja, A. Becker, A. Jaron-Becker, M. M. Murnane, and H. C. Kapteyn, Science **336**, 1287 (2012).
5. S. L. Cousin, F. Silva, S. Teichmann, M. Hemmer, B. Buades, and J. Biegert, Opt. Lett. **39**, 5383 (2014).
6. E. Seres, J. Seres, and C. Spielmann, Appl. Phys. Lett. **89**, 181919 (2006).
7. H. Fattahi, H. G. Barros, M. Gorjan, T. Nubbemeyer, B. Alsaif, C. Y. Teisset, M. Schultze, S. Prinz, M. Haefner, M. Ueffing, A. Alismail, L. Vámos, A. Schwarz, O. Pronin, J. Brons, X. T. Geng, G. Arisholm, M. Ciappina, V. S. Yakovlev, D.-E. Kim, A. M. Azzeer, N. Karpowicz, D. Sutter, Z. Major, T. Metzger, and F. Krausz, Optica **1**, 45 (2014).
8. O. H. Heckl, J. Kleinbauer, D. Bauer, S. Weiler, T. Metzger, and D. H. Sutter, *Ultrafast Thin-Disk Lasers* (Springer, 2016), pp. 93–115.
9. R. Fleischhaker, R. Gebs, A. Budnicki, M. Wolf, J. Kleinbauer, and D. H. Sutter, *Conference on Lasers & Electro-Optics Europe & International Quantum Electronics Conference* (CLEO, 2013), p. 1.
10. F. Röser, T. Eidam, J. Rothhardt, O. Schmidt, D. N. Schimpf, J. Limpert, and A. Tünnermann, Opt. Lett. **32**, 3495 (2007).
11. P. Russbueldt, T. Mans, G. Rotarius, J. Weitenberg, H. D. Hoffmann, and R. Poprawe, Opt. Express **17**, 12230 (2009).
12. C. Teisset, M. Schultze, R. Bessing, M. Häfner, J. Rauschenberger, D. Sutter, and T. Metzger, *Picosecond Thin-Disk Regenerative Amplifier with High Average Power for Pumping Optical Parametric Amplifiers* (OSA, 2013), paper CTh5C.6.
13. L. E. Zapata, H. Lin, A.-L. Calendron, H. Cankaya, M. Hemmer, F. Reichert, W. R. Huang, E. Granados, K.-H. Hong, and F. X. Kärtner, Opt. Lett. **40**, 2610 (2015).
14. J. Speiser, J. Opt. Soc. Am. B **26**, 26 (2009).
15. H. Fattahi, A. Schwarz, X. T. Geng, S. Keiber, D. E. Kim, F. Krausz, and N. Karpowicz, Opt. Express **22**, 31440 (2014).
16. C. J. Saraceno, F. Emaury, C. Schriber, M. Hoffmann, M. Golling, T. Südmeyer, and U. Keller, Opt. Lett. **39**, 9 (2014).
17. J. Brons, V. Pervak, E. Fedulova, D. Bauer, D. Sutter, V. Kalashnikov, A. Apolonskiy, O. Pronin, and F. Krausz, Opt. Lett. **39**, 6442 (2014).
18. D. Bauer, I. Zawischa, D. H. Sutter, A. Killi, and T. Dekorsy, Opt. Express **20**, 9698 (2012).
19. G. Arisholm, J. Opt. Soc. Am. B **14**, 2543 (1997).
20. D. Zhang, Y. Kong, and J.-Y. Zhang, Opt. Commun. **184**, 485 (2000).
21. K. Kato, IEEE J. Quantum Electron. **30**, 2950 (1994).
22. H. Fattahi, *Third-Generation Femtosecond Technology* (Springer, 2015).
23. T. Metzger, A. Schwarz, C. Y. Teisset, D. Sutter, A. Killi, R. Kienberger, and F. Krausz, Opt. Lett. **34**, 2123 (2009).
24. J. Fischer, A.-C. Heinrich, S. Maier, J. Jungwirth, D. Brida, and A. Leitenstorfer, Opt. Lett. **41**, 246 (2016).
25. H. Fattahi, A. Schwarz, S. Keiber, and N. Karpowicz, Opt. Lett. **38**, 4216 (2013).
26. A. Baltuška, T. Fuji, and T. Kobayashi, Phys. Rev. Lett. **88**, 133901 (2002).